

# An Analytical Model for the Reverse Link of WCDMA Systems With Repeaters in Nonuniform Traffic Distributions

Ferran Adelantado, *Member, IEEE*, Jordi Pérez-Romero, *Member, IEEE*, and Oriol Sallent

**Abstract**—The current extensive Third Generation network deployment has to cope with the existence of nonhomogeneous spatial traffic distributions, which are usually in the form of areas with high density of traffic. The concentration of users in some areas, particularly those far away from the base stations, can result in quality-of-service degradation due to high propagation losses. In this context, repeaters have turned out to be cost-effective nodes that are capable of mitigating these negative effects. This paper describes and models a multicellular/multiservice wideband code division multiple access system with repeaters in an environment with spatial nonuniformities. An analytical model is presented, and the expressions for the required transmission power, outage probability, and block error rate are derived for the reverse link. The implications of the noise amplification caused by the deployment of the repeaters as well as the variation of the propagation loss have been taken into account. Results focus on determining the maximum load factor for a given outage probability. In particular, special attention is paid to the effect of key parameters such as the gain between the base station and the repeaters, denoted as coupling gain, and the location of the different repeaters.

**Index Terms**—Load factor, nonuniformities, repeaters, service distribution, traffic distribution, WCDMA, wideband code division multiple access (WCDMA) capacity.

## I. INTRODUCTION

THE NETWORK deployment phase in a wireless system has two main design objectives: to provide reliable coverage to all users by minimizing the probability of coverage gaps and to maximize the capacity of the system so that services with high resource consumption requirements can be offered and more users can be allocated. Both objectives are tightly coupled in wideband code division multiple access (WCDMA)-based systems, and therefore, special care must be taken. Focusing on nonhomogeneous spatial traffic and service distributions, deployment solutions arise as feasible options to cope with the

degradation of the quality of service (QoS) that is typical in such scenarios. Accordingly, in the literature, we find several proposals involving microcells and repeaters [1], [2]. Microcells, as a part of a hierarchical cell structure [3], [4], have significantly higher capacity than macrocells and reduce power consumption in densely populated areas. In contrast, macrocells reduce the handover probability, particularly in those scenarios with high mobility users [5]. Cellular deployments including microcells have been studied in depth in terms of mobility [1], [5], handover [6], [7], power control [8], radio resource management (RRM) procedures [9], deployment [10], and cell boundaries [11], [12]. The deployment of a microcell implies a reduction of the path loss between the surrounding users and the serving node. When the microcell is located in the vicinity of areas with high density of traffic, it becomes the serving node of a high percentage of users, and the average path loss is reduced, thus leading to an increase in the capacity. Moreover, their deployment does not imply a significant increase in the interference, since transmission power levels are usually low. Despite the advantages provided by microcells in nonhomogeneous scenarios [9], [13], [14], repeaters have also been proposed as a cost-efficient solution. Although repeaters were first addressed to cover dead spots<sup>1</sup> [15], [16] (or particular cases such as indoor coverage with repeaters [17]), they are also appropriate to increase the capacity of areas with high density of traffic [18]–[20]. As with microcells, the inclusion of repeaters varies the parameters such as the statistics of distance between users and serving nodes or distance between serving nodes and interference sources. Repeaters, however, may cause undesired effects, such as noise amplification, particularly in the uplink (the aggregate of the thermal noise of all of the repeaters) [18]–[20]. Yet, it has been shown in the literature that an appropriate configuration increases the capacity of the system [18]. Some other studies on repeaters have been carried out by means of Monte Carlo simulations [21] or measurement campaigns [22], although there is no complete analytical model to analyze such situations.

The QoS level offered to users connected to the network does not only depend on the deployment configuration but also on the RRM strategies. Once the number of nodes and their locations have been determined, the dynamics of the network are monitored and controlled to maintain an appropriate QoS

Manuscript received March 7, 2007; revised July 19, 2008 and September 30, 2008. First published November 18, 2008; current version published May 11, 2009. This work was supported in part by the Spanish Research Council and in part by FEDER under COGNOS Grant TEC2007-60985. The review of this paper was coordinated by Prof. Y. Ma.

F. Adelantado was with the Universitat Politècnica de Catalunya, 08034 Barcelona, Spain. He is now with the Universitat Oberta de Catalunya, 08018 Barcelona, Spain.

J. Pérez-Romero is with the Department of Signal Theory and Communications, Universitat Politècnica de Catalunya, 08034 Barcelona, Spain.

O. Sallent is with the Universitat Politècnica de Catalunya, 08034 Barcelona, Spain.

Color versions of one or more of the figures in this paper are available online at <http://ieeexplore.ieee.org>.

Digital Object Identifier 10.1109/TVT.2008.2009541

<sup>1</sup>In the literature, dead spots are defined as areas with weak received RF signal energy.

level. In this context, the call admission control (CAC) is the first mechanism to avoid an excessive increase of the load. The basis of the mechanism is the following. First, a maximum load threshold ( $\eta_{\max}$ ) is set; then, all admission requests whose acceptance implies an increase of the load above  $\eta_{\max}$  are rejected. CAC has been studied thoroughly for macrocellular scenarios; however, the impact of repeaters on CAC has not yet been addressed.

This study is an improvement of a previous work where a single cell without repeaters was analyzed [23]. In the study presented in this paper, an analytical model to evaluate the effect of repeaters in a multicell/multiservice environment with traffic and service nonuniformities is developed. Furthermore, this model is useful for deriving the maximum acceptable load factor ( $\eta_{\max}$ ) required to prevent an overload that causes outage probability degradation. Then, the maximum load values are employed as inputs to tune the CAC. As aforementioned, there are some studies in the literature that focus on the analysis of scenarios with repeaters. Yet, the determination of the maximum allowable load factor ( $\eta_{\max}$ ) in such scenarios with traffic nonhomogeneities is not addressed in any of them.

The remainder of this paper is organized as follows. Section II characterizes the traffic and describes a generic scenario. In Section III, the analytical model is developed and expressions for block error rate (BLER) and outage probability are derived. Results obtained by means of the developed model and Monte Carlo simulations are shown in Section IV. Finally, conclusions are summarized in Section V.

## II. PROBLEM FORMULATION

### A. Traffic Characterization

Any complex scenario can always be split up into a set of simpler overlapped scenarios. This assertion is the basis of the traffic model considered in the study. Let a traffic layer be defined as each of the simple scenarios resulting from the splitting process. Any actual traffic scenario could be expressed as the sum of a set of layers. The splitting of a particular scenario can be performed according to a set of rules. In this case, the criterion is such that the traffic is uniformly distributed among the users distributed within each layer. Focusing on the study, the traffic of the proposed scenario is distributed among  $K$  circularly shaped layers ( $L_i, 0 \leq i \leq K-1$ ), each of which is characterized by the polar coordinates of the center ( $\delta_i, \theta_i$ ), the radius  $\rho_i$ , and the proportion of the total users within this layer  $\alpha_i$ . Let  $T_T$  denote the total number of users.  $T_T$  users are distributed among the  $K$  layers, and the proportion of users belonging to layer  $L_i$  is given by

$$\alpha_i = \frac{T_i}{T_T} \quad (1)$$

where  $T_i$  is the number of users within layer  $L_i$ . On the other hand,  $H$  possible services ( $0 \leq h \leq H-1$ ) are identified.  $s_{i,h}$  denotes the proportion of the total users with the  $h$ th service in layer  $L_i$ . In general, the traffic source is not continuously transmitting packets within a session, and some periods of

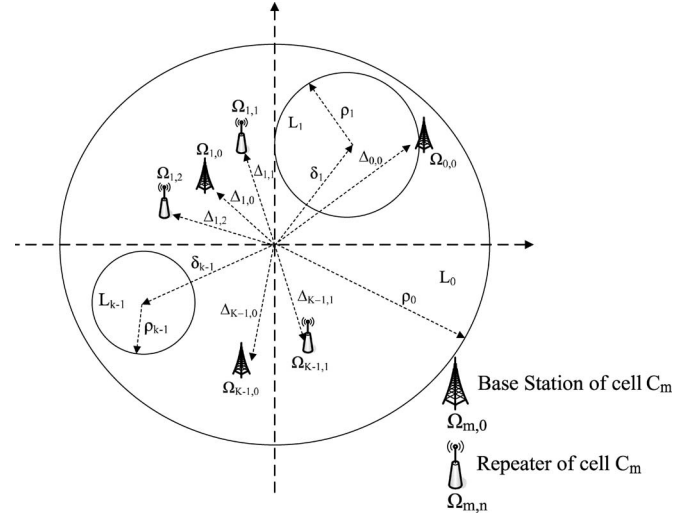


Fig. 1. Layout of a generic scenario with repeaters.

activity alternate with periods of inactivity (e.g., reading time during a WWW download or silence periods in speech calls). Then, the activity factor  $\varepsilon_h$  for the  $h$ th service is defined as the proportion of time in which a user is transmitting for this service, taking into account session and intersession time. With respect to periods of activity, in which a certain user is transmitting data through the air interface, there may exist several possibilities for each service to transmit the data flow, which are essentially characterized by a transmission bit rate ( $R_b$ ) and a required energy per bit to noise density ratio ( $E_b/N_0$ ). Following the Third Generation Partnership Project (3GPP) terminology [24], these possibilities will hereafter be denoted as transport format (TF).<sup>2</sup> The number of possible TFs for the  $h$ th service is denoted as  $TFS_h$ . The set of possible bit rates for the  $h$ th service is then  $R_{b_{h,j}} (0 \leq j \leq TFS_h - 1)$ , and the corresponding energy per bit to noise density ratio is  $(E_b/N_0)_{h,j}$  with  $0 \leq j \leq TFS_h - 1$ . Usually,  $SF_{h,j}$  (the spreading factor) is used instead of  $R_{b_{h,j}}$ , where  $SF_{h,j} = W/R_{b_{h,j}}$  ( $W$  is the total bandwidth).  $\chi_{h,j}$  is defined as the probability that the  $h$ th service uses the  $j$ th TF, which depends on the specific medium access control algorithm that executes the TF selection in the uplink (see, e.g., [25] for some examples).

### B. Description of the Scenario

The whole scenario is divided into  $M$  cells ( $C_m, 0 \leq m \leq M-1$ ). Each of these cells can be composed of more than a single node. Thus, cell  $C_m$  has  $N_m$  nodes, each one denoted as  $\Omega_{m,n} (0 \leq n \leq N_m - 1)$ . In any case,  $\Omega_{m,0}$  is always the base station of the cell  $C_m$ , whereas the rest  $\Omega_{m,n} (n \neq 0)$  are repeaters. These nodes (a base station and  $N_m - 1$  repeaters) are also characterized by their location with respect to the origin of the coordinates: the distance to the origin ( $\Delta_{m,n}$ ) and the angle with the axis ( $\Theta_{m,n}$ ), where  $m$  is the cell to which they belong, and  $n$  the node identifier (Fig. 1).

<sup>2</sup>Note that, although the 3GPP terminology is used here, the concept of TFs would be general to any WCDMA system with a variable transmission bit rate.

Until now, the topology of the system has been characterized in terms of cells and nodes. Each cell is composed of a number of nodes (i.e., one base station and a number of repeaters) and geographically corresponds to the coverage area provided by these nodes. In turn, the layers determine the spatial distribution of the traffic generated by the users in the whole scenario (i.e., each layer is assumed to be a circular area with a certain user density with different services). Notice that there is no direct correspondence between cells and traffic layers, which means that, inside the coverage area of one cell, there can be any number of traffic layers.

All repeaters of a particular cell ( $\Omega_{m,n}$  with  $1 \leq n \leq N_m - 1$ ) are connected to the base station ( $\Omega_{m,0}$ ) through a radio link [26]. Each base station–repeater link is characterized by propagation losses (including all effects derived from radio interface) and the gain of the antennas. The final coupling gain between the donor base station and the  $n$ th repeater is denoted as  $\phi_{m,n}$ . Taking into account that  $\Omega_{m,0}$  is the base station of cell  $C_m$ ,  $\phi_{m,0} = 0$  dB.

To achieve optimum performance from repeaters, antennas at the repeater and base station must be installed under line-of-sight conditions. Therefore, directive-type antennas can be used at both ends.

The isolation between these two antennas plays a key role in the performance of the repeater, since it is necessary to guarantee the stability of the repeater. For instance, in [27], the minimum required isolation according to the different repeater parameters is defined for the Universal Mobile Telecommunications System (UMTS). In this study, perfect isolation is assumed. Furthermore, repeater requirements in terms of spurious levels, frequency stability, and test conditions are also taken into account (e.g., [28] and [29] defined these requirements for UMTS).

Thermal noise is another crucial aspect in the performance of the system when one or several repeaters are deployed within a cell. Let  $P_{N_{m,n}}^{UL}$  be the noise power of node  $\Omega_{m,n}$ . The total uplink noise power of the cell  $C_m$  is then the sum of the contributions of  $\Omega_{m,0}$  and of all the repeaters connected [16].

$$P_{N_m}^{UL} = \sum_{n=0}^{N_m-1} \phi_{m,n} P_{N_{m,n}}^{UL}. \quad (2)$$

In fact, the increase of the uplink noise figure caused by repeaters (which are usually noisier than base stations) turns the uplink into a bottleneck. Hereafter, the noise power of repeaters will be expressed with respect to the base station noise power. The uplink thermal noise power of node  $n$  is expressed as  $P_{N_{m,n}}^{UL} = \beta_{m,n} P_{N_{m,0}}^{UL}$ , where  $P_{N_{m,0}}^{UL}$  is the thermal noise power of the base station  $\Omega_{m,0}$  ( $\beta_{m,0} = 1.0$ ). Usually, repeaters tend to be noisier than base stations, and therefore,  $\beta_{m,n} \geq 1$  for  $n > 0$ .

Also noteworthy is the combination of the received signals. In this paper, only the uplink is discussed. The signal from the user is received at both the repeater and the base station. In some studies, a perfect combination of the signals is assumed. Therefore, considering a cell composed of a base station and

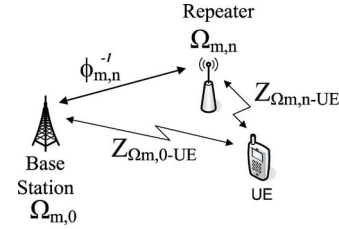


Fig. 2. Scheme of the propagation losses.

$N_m - 1$  repeaters, the received power at cell  $C_m$  from generic user equipment located within the scenario is computed as

$$\begin{aligned} P_{R_m} &= P_{T_m} \sum_{n=0}^{N_m-1} \phi_{m,n} Z_{\Omega_{m,n}}^{-1} \\ &= P_{T_m} \sum_{n=0}^{N_m-1} Z_{m,n}^{-1} \end{aligned} \quad (3)$$

where  $P_{R_m}$  is the power received at cell  $C_m$  from the generic user,  $P_{T_m}$  is the user equipment transmission power, and  $Z_{\Omega_{m,n}}$  is the total propagation loss between node  $\Omega_{m,n}$  and the user (see Fig. 2). Note that, for the sake of simplicity, all user subscripts have been omitted, since the notation always refers to a generic user.

We denote  $h_{m,n}$  as the channel gain from the mobile user to the base station through the node  $\Omega_{m,n}$ ,  $h_{m,n} = Z_{m,n}^{-1}$ .

Although the sum of the contributions increases the received power, it is not convenient to assume that there is a perfect combination of the direct signal and the signal received through the repeaters. These signals present different delays, and they can only be combined if those delay differences are small enough. For instance, the 3GPP standard [27] points out that the resolvable multipaths are lower for repeaters than for macrocellular deployment. It is worth noting that considering the perfect combination of base station and repeater signals would be the most optimistic approach. Consequently, in order to avoid an overestimation of the capacity of the system with repeaters, this study assumes that only one of the signals is useful, either the one from the repeater or the one from the mobile user. Therefore, making use of the same notation used so far, the received power is as follows [30]:

$$P_{R_m} = \frac{P_{T_m}}{Z_m} \quad (4)$$

where  $Z_m = \min(Z_{m,n}) \forall n \in [0, \dots, N_m - 1]$ . The importance of deploying repeaters stems from the decrease of propagation losses, since the mobile user will always be connected to the cell through the path with minimum loss.

### III. ANALYTICAL MODEL

Communication systems are usually characterized by QoS parameters such as outage probability or BLER. In this context, the analytical model developed in this paper is intended to derive the expression of such parameters for the scenario described in Section II-B.

The impact of multicell nonuniformly distributed traffic scenarios can be found in terms of the required transmission power or, in other words, in terms of the outage probability, because a

user will be in outage whenever it has not enough transmission power to satisfy the signal to interference and noise ratio requirements. The required uplink transmission power for a user connected to cell  $C_m$  through any of the nodes is as follows [25]:

$$P_{T_m} \text{ (dBm)} = Z_m + 10 \log \left( \frac{P_{N_{m,0}}^{\text{UL}} \sum_{n=0}^{N_m-1} \beta_{m,n} \phi_{m,n}}{(1 - \eta_m) \left( \frac{W}{\left( \frac{E_b}{N_0} \right) R_b} + 1 \right)} \right) = Z_m + \Phi_m \quad (5)$$

where  $W$  is the total bandwidth and  $\eta_m$  is the uplink load factor. The load factor ( $\eta_m$ ) [31] stands for the theoretical spectral efficiency of a WCDMA cell, i.e., the proportion of the total interference with respect to the total interference plus thermal noise. It ranges from 0 to 1 (from low to high load, respectively), and it is calculated as

$$\eta_m = 1 - \frac{P_{N_{m,0}}^{\text{UL}} \sum_{n=0}^{N_m-1} \beta_{m,n} \phi_{m,n}}{P_{N_{m,0}}^{\text{UL}} \sum_{n=0}^{N_m-1} \beta_{m,n} \phi_{m,n} + I_m^{\text{OWN}} + I_m^{\text{OTHER}}} \quad (6)$$

where  $I_m^{\text{OWN}}$  and  $I_m^{\text{OTHER}}$  stand for the interference received at cell  $C_m$  from the cell itself and from other cells, respectively.

As displayed in (5), the required transmission power in the uplink depends on  $Z_m$  and  $\Phi_m$ . As for  $\Phi_m$ , it reflects the effect of thermal noise, interference, and QoS requirements on the required transmission power. Thus, it grows as the total loss, the thermal noise power (the contributions of all the nodes in the cell), the QoS parameters (transmission rate and energy per bit to noise density ratio), and/or the load factor increases, and so does  $P_{T_m}$ .

Note that spatial nonhomogeneities in the traffic distribution do affect the distribution of path loss in the cell [32]. Therefore, it is necessary to compute these statistics in order to analyze the implications of the traffic distribution on propagation losses. Any location in the scenario shown in Fig. 1 is characterized by the distance to the origin ( $r$ ) and the angle ( $\theta$ ). In particular, the distance and the angle probability density functions (pdfs) of layer  $L_i$  are denoted as  $f_R^i(r)$  and  $f_\theta^i(\theta)$ , respectively, and are computed in Appendix I.

Both random variables, distance and angle, are independent. Therefore, as traffic is distributed among  $K$  layers, each of them with a proportion of the total number of users equal to  $\alpha_i$ , the total pdf is

$$f_{R,\theta}(r, \theta) = \sum_{i=0}^{K-1} \alpha_i f_R^i(r) f_\theta^i(\theta) = \sum_{i=0}^{K-1} \alpha_i f_{R,\theta}^i(r, \theta) \quad (7)$$

where  $f_{R,\theta}^i(r, \theta)$  is the joint pdf of the  $i$ th traffic layer. The total loss observed by users with respect to cell  $m$  through node  $n$  is computed as

$$Z_{m,n} \text{ (in decibels)} = Y_0 + \zeta \log r_{m,n} + S_{m,n} - \phi_{m,n} \quad (8)$$

where  $Y_0$  and  $\zeta$  are environment constants,  $r_{m,n}$  is the distance from node  $\Omega_{m,n}$  to the user location, and  $S_{m,n}$  is the lognormal shadowing expressed in decibels.

Then, according to the definitions already stated, the probability distribution function of the total loss of cell  $C_m$  is given by

$$F_{Z_m}(z) = \int_0^\infty \int_0^{2\pi} f_{R,\theta}(r, \theta) P(Z_m \leq z) d\theta dr. \quad (9)$$

All the parameters that describe the scenario in terms of traffic and deployment layout are involved in the calculation of  $F_{Z_m}(z)$ . The mathematical development of  $P(Z_m \leq z)$  can be found in Appendix II. Finally,  $f_{Z_m}(z)$  may be obtained by deriving  $F_{Z_m}(z)$

$$f_{Z_m}(z) = \sum_{i=0}^{K-1} \lambda_{m,i} f_{Z_m}^i(z) \quad (10)$$

where  $f_{Z_m}^i(z)$  is the total propagation loss pdf of traffic layer  $L_i$  and is given by

$$f_{Z_m}^i(z) = \sum_{n=0}^{N_m-1} \int_0^\infty \int_0^{2\pi} f_{R,\theta}^i(r, \theta) \frac{\vartheta_{m,n}}{\varphi_m} d\theta dr \quad (11)$$

with

$$\lambda_{m,i} = \frac{\alpha_i \int_0^\infty \int_0^{2\pi} f_{R,\theta}^i(r, \theta) \varphi_m d\theta dr}{\sum_{s=0}^{K-1} \alpha_s \int_0^\infty \int_0^{2\pi} f_{R,\theta}^s(r, \theta) \varphi_m d\theta dr} \quad (12)$$

$$\vartheta_{m,n} = \frac{e^{-\frac{(z + \phi_{m,n} - Y_0 - \zeta \log(r_{m,n}))^2}{2\sigma_{S_{m,n}}^2}}}{\sqrt{2\pi} \sigma_{S_{m,n}}} \prod_{w=0}^{M-1} \prod_{\substack{l=0 \\ (w,l) \neq (m,n)}}^{N_w-1} \Xi_m^{w,l} \quad (13)$$

$$\Xi_m^{w,l} = Q \left( \frac{z + \phi_{w,l} - Y_0 - \Delta P_{P_{m,w}} - \zeta \log(r_{w,l})}{\sigma_{S_{w,l}}} \right) \quad (14)$$

$$\varphi_m = \sum_{n=0}^{N_m-1} \int_{-\infty}^\infty \frac{e^{-\frac{s_{m,n}^2}{2\sigma_{S_{m,n}}^2}}}{\sqrt{2\pi} \sigma_{S_{m,n}}} \prod_{w=0}^{M-1} \prod_{\substack{l=0 \\ (w,l) \neq (m,n)}}^{N_w-1} \Lambda_{m,n}^{w,l} dS_{m,n} \quad (15)$$

$$\Lambda_{m,n}^{w,l} = Q \left( \frac{S_{m,n} - B_{m,n}^{w,l} - A_{m,n}^{w,l} - \Delta P_{P_{m,w}}}{\sigma_{S_{w,l}}} \right) \quad (16)$$

where  $A_{m,n}^{w,l} = \phi_{m,n}$  (in decibels)  $- \phi_{w,l}$  (in decibels),  $\Delta P_{P_{m,w}} = P_{P_m} - P_{P_w}$ , and  $B_{m,n}^{w,l} = \zeta \log(r_{w,l}/r_{m,n})$ .  $P_{P_m}$  and  $P_{P_w}$  are the pilot powers transmitted by cells  $C_m$  and  $C_w$ , respectively (expressed in logarithmic units).

It may be observed from (5) that the required transmission power also depends on  $\Phi_m$ . In the case of WCDMA-based systems, only transmitting users (i.e., during periods of activity) contribute to an increase in the interference. Taking

this fact into account, the influence of each user on the total interference depends on the activity factor ( $\varepsilon_h$ ), the probability of selecting the  $j$ th TF of the  $h$ th service ( $\chi_{h,j}$ ), and the distribution of services within the layers ( $\varsigma_{i,h}$ ). As the selection of each TF for a specific service is a random variable, the probability function of  $\Phi_m$  for the traffic layer  $L_i$  in cell  $C_m$  is given by

$$P_{\Phi_m}^i(\Phi_m = \Phi_{h,j}) = \frac{U_{h,j,i}}{\sum_{q=0}^{H-1} \sum_{s=0}^{K-1} \lambda_{m,s} \varepsilon_q \varsigma_{s,q}} \quad (17)$$

where  $\Phi_{h,j}$  is defined as

$$\Phi_{h,j} = 10 \log \left( \frac{P_{N_m}^{UL}}{(1 - \eta_m) \left( \frac{W}{\left( \frac{E_b}{N_0} \right)_{h,j} R_{b,h,j}} + 1 \right)} \right) \quad (18)$$

$$U_{h,j,i} = \lambda_{m,i} \varepsilon_h \varsigma_{i,h} \chi_{h,j}. \quad (19)$$

Equation (17) is defined in a discrete probability space  $\mathcal{U}_\Phi = \{\Phi_{0,0}, \Phi_{0,1}, \dots, \Phi_{H-1, TFS_{H-1}}\}$ .

Finally, for a given load factor, the required transmission power density function is obtained by convoluting the  $Z_m$  and  $\Phi_m$  pdfs

$$f_{P_{T_m}}(P_{T_m}) = \frac{\sum_{h=0}^{H-1} \sum_{j=0}^{TFS_h-1} \sum_{i=0}^{K-1} U_{h,j,i} f_{Z_m}^i(P_{T_m} - \Phi_{h,j})}{\sum_{h=0}^{H-1} \sum_{i=0}^{K-1} \lambda_{m,i} \varepsilon_h \varsigma_{i,h}}. \quad (20)$$

The QoS performance in terms of outage probability ( $\mu_m$ ) and BLER may be extracted from the previous model. If an ideal power control is assumed, the transmission power will be equal to the required transmission power, provided that it is within the range  $[P_{T_{\min}}, P_{T_{\max}}]$ . A user is said to be in outage whenever the measured ( $E_b/N_0$ ) is below the target  $(E_b/N_0)_T$ , or equivalently, when  $P_{T_m}$  is above  $P_{T_{\max}}$ , the outage probability ( $\mu_m$ ) may be expressed as

$$\mu_m = P \left( \left( \frac{E_b}{N_0} \right) < \left( \frac{E_b}{N_0} \right)_T \right) = P(P_{T_m} > P_{T_{\max}}). \quad (21)$$

For a given load factor, the outage probability is then

$$\begin{aligned} \mu_{m,\eta_m} &= \int_{P_{T_{\max}}}^{\infty} f_{P_{T_m}}(P_{T_m}) dP_{T_m} \\ &= \frac{\sum_{h=0}^{H-1} \sum_{j=0}^{TFS_h-1} \sum_{i=0}^{K-1} U_{h,j,i} \int_{P_{T_{\max}}}^{\infty} f_{Z_m}^i(P_{T_m} - \Phi_{h,j}) dP_{T_m}}{\sum_{h=0}^{H-1} \varepsilon_h \sum_{i=0}^{K-1} \lambda_{m,i} \varsigma_{i,h}}. \end{aligned} \quad (22)$$

Likewise, BLER is defined as the percentage of erroneous blocks received at the base station. BLER is a function of  $(E_b/N_0)$  and depends on physical layer aspects, like channel coding, modulation, interleaving, etc. On the other hand, the measured  $(E_b/N_0)$  depends on the required transmission power [23]. Therefore, BLER is a function of the required transmission power

$$BLER_m = v_{h,j} \left( \left( \frac{E_b}{N_0} \right) \right) = \Upsilon_{h,j}(P_{T_m}) \quad (23)$$

where functions  $v_{h,j}()$  and  $\Upsilon_{h,j}()$  are specific for each service and TF. It is noteworthy that the relationship between BLER and  $(E_b/N_0)$  [the function  $v_{h,j}()$ ] is not a result from the model. It is assumed to be known *a priori* and used as an input. In particular, for a given load factor, BLER is expressed as (24), shown at the bottom of the page.

Additionally, outage probability and BLER may be computed for a specific layer or service. For instance, the outage probability for layer  $L_i$  [(25)] and service  $h$  [(26)] are shown in the following. BLER expressions are analogous.

$$\mu_{m,\eta_m}^i = \frac{\sum_{h=0}^{H-1} \sum_{j=0}^{TFS_h-1} \frac{U_{h,j,i}}{\lambda_{m,i}} \int_{P_{T_{\max}}}^{\infty} f_{Z_m}^i(P_{T_m} - \Phi_{h,j}) dP_{T_m}}{\sum_{h=0}^{H-1} \varepsilon_h \varsigma_{i,h}} \quad (25)$$

$$\mu_{m,\eta_m,h} = \frac{\sum_{j=0}^{TFS_h-1} \sum_{i=0}^{K-1} \frac{U_{h,j,i}}{\varepsilon_h} \int_{P_{T_{\max}}}^{\infty} f_{Z_m}^i(P_{T_m} - \Phi_{h,j}) dP_{T_m}}{\sum_{i=0}^{K-1} \lambda_{m,i} \varsigma_{i,h}}. \quad (26)$$

$$\begin{aligned} BLER_{m,\eta_m} &= \int_{-\infty}^{\infty} \Upsilon(P_{T_m}) f_{P_{T_m}}(P_{T_m}) dP_{T_m} \\ &= \frac{\sum_{h=0}^{H-1} \sum_{j=0}^{TFS_h-1} \sum_{i=0}^{K-1} U_{h,j,i} \int_{-\infty}^{\infty} \Upsilon_{h,j}(P_{T_m}) f_{Z_m}^i(P_{T_m} - \Phi_{h,j}) dP_{T_m}}{\sum_{h=0}^{H-1} \varepsilon_h \sum_{i=0}^{K-1} \lambda_{m,i} \varsigma_{i,h}} \end{aligned} \quad (24)$$

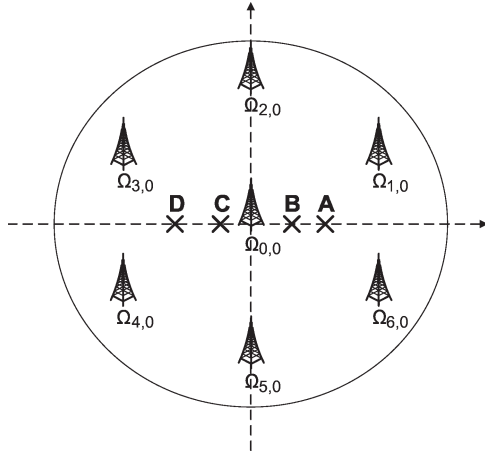


Fig. 3. Locations defined in the scenario.

TABLE I  
LOCATION PARAMETERS

Location	$\Delta$ (m)	$\Theta$ (rad)
A	850	0
B	550	0
C	550	$\pi$
D	850	$\pi$

IV. RESULTS

In this section, some scenarios are analyzed in order to highlight the impact of deploying repeaters. Each scenario is composed of a central cell (where all results are collected) and six neighboring cells that make up the first interference ring. The distance between neighboring base stations is 2000 m. Four possible locations for the repeater (A, B, C, and D) are shown in Fig. 3 and listed in Table I. A, B, C, and D are located on the horizontal axis for the sake of simplicity, although they could have different angles.

The parameters for all base stations and for the propagation model are listed in Table II. With regard to traffic distribution, two layers are considered. The first one has a radius  $\rho_0 = 3000$  m and is centered at the origin of the coordinates ( $\delta_0 = 0$  m). The second traffic layer has a radius  $\rho_1 = 100$  m, and its distance to the base station will be varied throughout this section. The parameters of the two services considered are listed in Table III. Fifty percent of the users will employ service 1, and 50% will employ service 2, in both traffic layers. In service 1, the first three TFs are used with a probability equal to 0.2 ( $\chi_{1,0} = \chi_{1,1} = \chi_{1,2} = 0.2$ ), whereas the last TF has a probability  $\chi_{1,3} = 0.4$ .

The physical layer has been characterized by means of the functions  $v_{n,j}()$  shown in Fig. 4. The curves shown in Fig. 4 have been obtained by means of a link level simulator that includes a 1500-Hz closed-loop power control, 1/3 turbo coding effect, and channel impulse response estimation.

The traffic layer  $L_0$  contains 90% of the users, and the rest of the users are scattered on layer  $L_1$  ( $\alpha_1 = 0.1$ ). Traffic layer  $L_1$  is located in A. Therefore, the area where  $L_1$  is located becomes an area with high density of traffic: 90% of the users

TABLE II  
SCENARIO PARAMETERS

Parameter	Value
$P_{N_{0,0}}^{UL}$	-103 dBm
$Y_0$	128.1
$\zeta$	37.6
$\sigma_S$	3 dB
$P_{T_{max}}$	21 dBm
$P_{T_{min}}$	-44 dBm
$\Delta_{0,0}$	0 m
$\Theta_{0,0}$	0 rad
$\Delta_{m,0} \{\forall m \in [1, 6]\}$	2000 m
$\Theta_{m,0} \{\forall m \in [1, 6]\}$	$\frac{\pi}{3}(m-1) + \frac{\pi}{6}$ rad

TABLE III  
PARAMETERS OF SERVICES 0 AND 1

Service 0		Service 1	
Parameter	Value	Parameter	Value
$\varepsilon_0$	0.5	$\varepsilon_1$	0.8
TFS <sub>0</sub>	1	TFS <sub>1</sub>	4
$R_{b_{0,0}}$	64 kbps	$R_{b_{1,0}}$	12.2 kbps
$\left(\frac{E_b}{N_0}\right)_{0,0}$	4 dB	$\left(\frac{E_b}{N_0}\right)_{1,0}$	5 dB
		$R_{b_{1,1}}$	32 kbps
		$\left(\frac{E_b}{N_0}\right)_{1,1}$	5 dB
		$R_{b_{1,2}}$	64 kbps
		$\left(\frac{E_b}{N_0}\right)_{1,2}$	5 dB
		$R_{b_{1,3}}$	128 kbps
		$\left(\frac{E_b}{N_0}\right)_{1,3}$	5

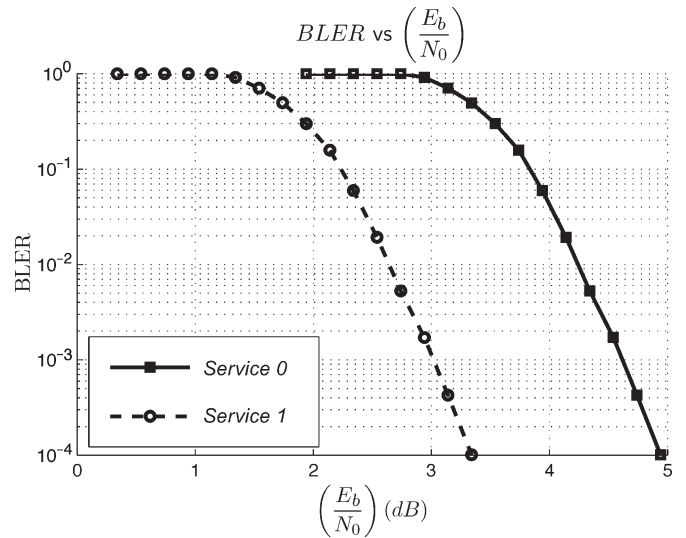


Fig. 4. Services' BLER versus  $(E_b/N_0)$ .

are uniformly scattered around the whole scenario (the area covered by  $L_0$ ). The remaining 10% of users are spread out within  $L_1$ ; therefore, in the area covered by  $L_1$ , there is the sum of the contributions of the two layers (all users within  $L_1$  and the proportional part of  $L_0$ ). The maximum tolerable outage probability ( $\mu_{max}$ ) is set to 2%, and the associated  $\eta_{max}$  is analyzed when a repeater with  $\beta_{0,0} = 1.0$  (0 dB) is set up in location A, B, C, or D.

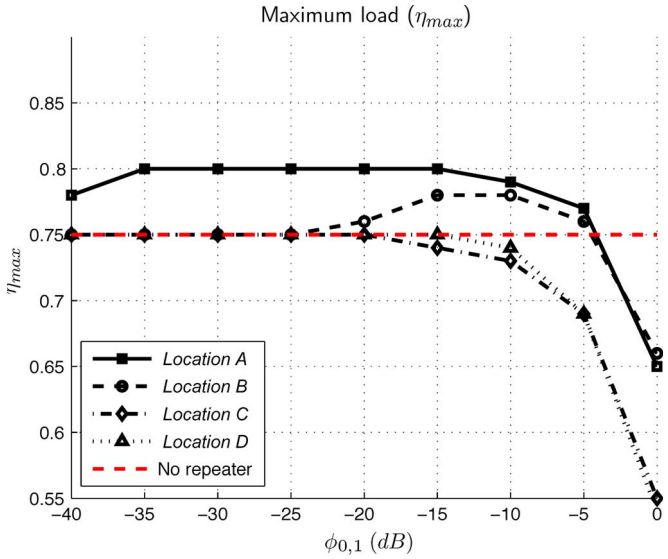


Fig. 5. Maximum load associated with a 2% outage probability as a function of the coupling gain.

The analysis of the results has been divided into three different stages. First, in Section IV-A, the influence of the coupling gain on the load factor threshold is studied. In the second step (Section IV-B), the importance of the location of the repeaters is analyzed. Finally, in the last section, the capacity of the scenario in terms of users is also obtained.

A. Effect of the Coupling Gain

Fig. 5 shows the evolution of  $\eta_{max}$  as a function of the coupling gain ( $-40 \text{ dB} \leq \phi_{0,1} \leq 0 \text{ dB}$ ). It is worth noting that the maximum allowable load factor grows as the repeater is placed closer to the area with high density (i.e., the layer  $L_1$  in location A). It is also clear that, for high coupling gains, the increase in noise caused by the repeater results in low  $\eta_{max}$  values. Yet, when the coupling gain ( $\phi_{0,1}$ ) is decreased, the decrease of the total loss of the users connected to the repeater compensates the effect of the noise amplification. Hence,  $\eta_{max}$  reaches its maximum. After the maximum,  $\eta_{max}$  begins to decrease. All load curves tend to the same value for low coupling gains. In fact, the lower the coupling gain is, the fewer users will be connected to the cell through the repeater, and therefore, the more similar the total loss pdf will be with respect to the case without a repeater. Likewise, the thermal noise of the repeater will also be attenuated by this gain. The combination of these two factors implies that the effect of deploying repeaters tends to vanish as the coupling gain decreases. Yet, the speed with which the effect vanishes depends on the configuration of the scenario (number, location and gain of the repeaters, and traffic distribution).

Consider the scenario where both layer  $L_1$  and repeater  $\Omega_{0,1}$  are located in A; for the traffic distribution,  $\alpha_1$  is varied from 0.1 to 0.3 (and consequently,  $\alpha_0$  varies from 0.9 to 0.7). Fig. 6 shows the evolution of  $\eta_{max}$  in this case. The results reveal that the higher  $\alpha_1$  is, the higher  $\eta_{max}$  is. In fact, combining the results observed in Figs. 5 and 6, it is clear that the distance of

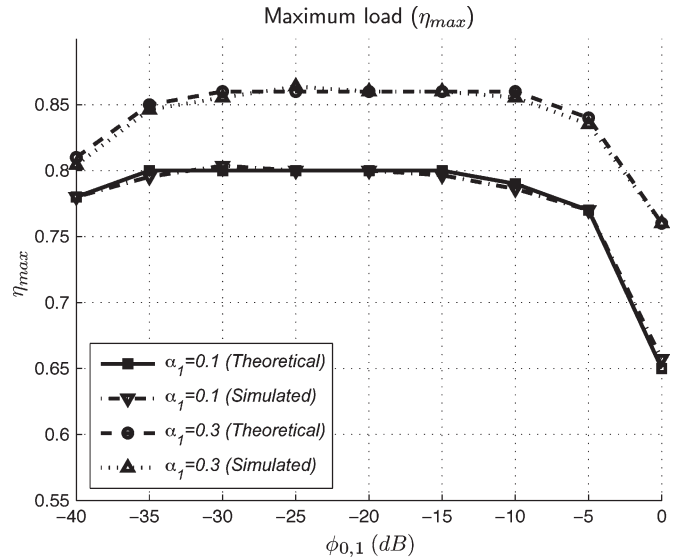


Fig. 6. Maximum load associated with a 2% outage probability for different traffic distributions.

users to the node by which they are served becomes a determinant parameter. Thus, when repeaters are located close to areas with high density of traffic, the maximum load factor grows as the concentration of users is increased (i.e., the average distance to the serving node decreases).

In order to check the accuracy of the model, results obtained from simulations have also been included in Fig. 6. Simulations have been carried out by using the Monte Carlo method. Assuming a given load factor, a number of mobile users are successively located in the scenario, and the outage probability is computed. This process is repeated for different load factor values until the target outage probability (2%) is reached. The figure shows that the model and the derived expressions accurately represent the performance of the system.

The noise factor of the repeater is important in this kind of scenarios. Because the noise power is received at the base station through the radio link, the attenuation suffered by the signal is also suffered by the noise and the interference. Therefore, noisy repeaters can deteriorate the features of the system.

B. Effect of the Repeater Location

In the previous results, the traffic layer  $L_1$  was located in A. Now, this traffic layer is moved toward the base station and located in B (see Fig. 3). Fig. 7 shows the effect of the repeater location on the maximum load factor as a function of the coupling gain. It may be observed that, in this case, when a repeater is deployed, the improvement achieved in terms of maximum load is significantly slighter (compared to results shown in Fig. 5). Consequently, the effectiveness of the repeater deployment strategy to increase the capacity (in terms of load factor) is tightly coupled with the distance between the base station and the repeater. In particular, the improvement in the capacity is higher as the distance grows.

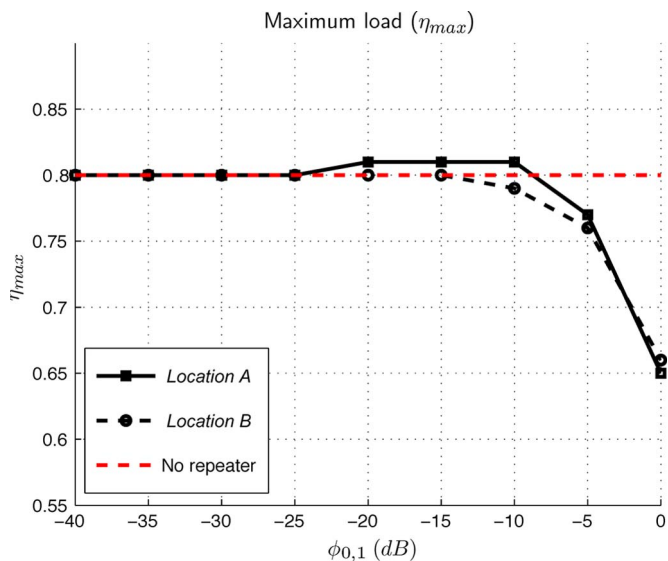


Fig. 7. Maximum load factor when  $L_1$  is in B and the repeater is located in A or B.

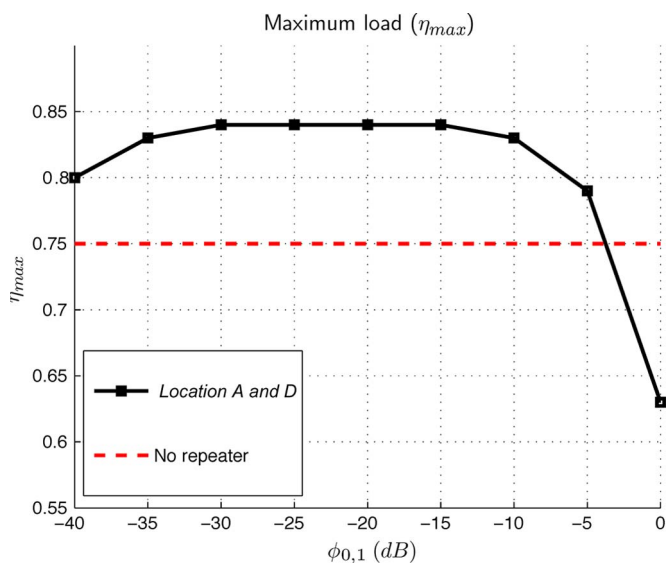


Fig. 8. Maximum load with two repeaters and two high-traffic-density areas.

So far, the evolution of the load factor in single-repeater scenarios has been analyzed. However, the number of repeaters is not necessarily limited to one. Consider a scenario with three traffic layers; the first layer is  $L_0$  with  $\alpha_0 = 0.8$ , the second layer is  $L_1$  with  $\alpha_1 = 0.1$  and is located in A, and finally, the third layer  $L_2$  is located in D and has  $\alpha_2 = 0.1$ . Likewise, two repeaters are deployed, one in A and the other one in D. The result obtained is shown in Fig. 8. The increase in the maximum load over 0.8 (the value obtained in the same scenario but without repeaters) is remarkable. It is true that the noise power level grows as the number of repeaters is increased; however, the reduction of the distance between users and nodes contributes to the increase of the maximum load factor.

The situation analyzed in Fig. 8 is appropriate, since repeaters share their locations with high traffic areas, but the

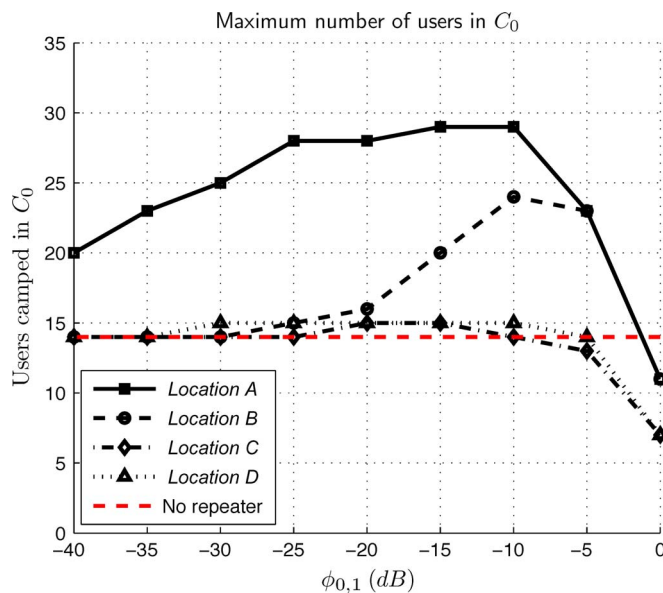


Fig. 9. Maximum number of users camped in  $C_0$  that could be admitted in order to keep the outage probability below 2%.

maximum load level will decrease or increase depending on how far these repeaters are deployed from these areas and the density of these areas with high density of traffic themselves.

### C. Capacity Results

The relationship between the number of users connected to a cell and the load factor of this cell is highly dependent on the distribution of the users and services as well as on the parameters of all the nodes in the scenario (base stations and repeaters). Hence, the maximum capacity of the cell for a given maximum outage probability must be obtained by means of Monte Carlo simulations. The scenario considered here is the same as the one used in the previous section, with  $L_1$  located in A,  $\alpha_0 = 0.9$ , and  $\alpha_1 = 0.1$ . Fig. 9 shows the same results presented in Fig. 5 but in terms of users<sup>3</sup> instead of considering them in terms of load factor. It has already been observed that the relationship between users and the load factor is not straightforward. This nonlinearity notwithstanding, the shapes of both curves follow the same trend, and thus, higher loads are translated into a higher number of users. Once again, it is shown that the maximization of the capacity is achieved when repeaters are located close to areas with high density of traffic. Moreover, it should be noted that high coupling gains (e.g.,  $\phi_{0,1} = 0$  dB) cause negative effects in terms of capacity. In fact, high coupling gain values increase the coverage area of the cell although they introduce high noise levels.

## V. CONCLUSION

An analytical model has been proposed to evaluate the maximum allowable uplink load factor in a multicell/multiservice

<sup>3</sup>Results are expressed in terms of camped users. Camped users are defined as the users served by the cell without distinguishing whether they are transmitting or not.

WCDMA scenario that includes repeaters and nonuniform traffic spatial distributions. The outage probability as a function of the load factor has been obtained in order to assess the appropriate maximum admission load in the scenarios described. It has been shown that the proper selection of the load threshold ( $\eta_{\max}$ ) depends on traffic and service distribution parameters as well as on the deployment of the network. The study has been divided into two parts: the first part provides insight into the maximum load factor ( $\eta_{\max}$ ) determination by making use of the analytical model, whereas the second part relates the maximum allowable load factor to the maximum number of users. The most important conclusion extracted from the results is that, although it is possible to improve the capacity of the cell by deploying repeaters, the performance of the system is extremely sensitive to the locations of the repeaters as well as to their parameters (noise figure and coupling gain). The noise level observed at the cell is the sum of the noise introduced by each node of the cell weighted by the corresponding coupling gain ( $\phi_{m,i}$ ). Therefore, there is a tradeoff regarding the coupling gain: the higher is the coupling gain, the lower is the power that users need to transmit. However, high coupling gain values mean high noise contributions. Consequently, the repeater should be placed in the same locations as areas with high density of traffic to compensate for the increase in the noise with a high decrease in the average propagation loss. Furthermore, the improvement is higher as the distance between the areas with high density of traffic and the base station increases.

#### APPENDIX I

The analysis of the distance and angle pdfs [ $f_R^i(r)$  and  $f_\theta^i(\theta)$ ] of a generic circularly shaped layer  $L_i$  with radius  $\rho_i$  and a distance to the origin  $\delta_i$  (see Fig. 1) presents two different cases: when the origin of the coordinates is located within the  $i$ th layer ( $\delta_i \leq \rho_i$ ) and when it is not ( $\delta_i > \rho_i$ ).

1) If  $\delta_i \leq \rho_i$

$$f_\theta^i(\theta) = \frac{1}{\pi\rho_i^2} \times \left[ \delta_i^2 \cos(\theta - \theta_i) + \frac{\rho_i^2 - \delta_i^2}{2} + \frac{\delta_i^2 \cos(\theta - \theta_i)}{\sqrt{\left(\frac{\rho_i}{\delta_i}\right)^2 - \sin(\theta - \theta_i)}} \right] 0 \leq \theta \leq 2\pi. \quad (27)$$

a) If  $0 \leq r \leq \rho_i - \delta_i$

$$f_R^i(r) = \frac{2r}{\rho_i^2}. \quad (28)$$

b) If  $\rho_i - \delta_i < r \leq \rho_i + \delta_i$

$$f_R^i(r) = \frac{1}{\pi\rho_i^2} \left[ \pi r - 2r \arcsin \frac{\delta_i^2 + r^2 - \rho_i^2}{2\delta_i r} \right] \quad (29)$$

2) If  $\delta_i > \rho_i$

$$f_R^i(r) = \frac{1}{\pi\rho_i^2} \left[ \pi r - 2r \arcsin \frac{\delta_i^2 + r^2 - \rho_i^2}{2\delta_i r} \right] \delta_i - \rho_i < r_i \leq \delta_i + \rho_i \quad (30)$$

$$f_\theta^i(\theta) = \frac{2}{\pi} \left( \frac{\delta_i}{\rho_i} \right)^2 \cos(\theta - \theta_i) \sqrt{\left( \frac{\rho_i}{\delta_i} \right)^2 - \sin(\theta - \theta_i)} \theta_{i,0} \leq \theta \leq \theta_{i,1}. \quad (31)$$

#### APPENDIX II

For any pair of nodes  $\Omega_{m,n}$  and  $\Omega_{w,l}$  of the generic cells  $C_m$  and  $C_w$ , respectively, a user will be connected to  $\Omega_{m,n}$  only if

$$P_{P_m} - Z_{m,n} > P_{P_w} - Z_{w,l} \quad (32)$$

where  $P_{P_m}$  and  $P_{P_w}$  are the pilot powers transmitted by cells  $C_m$  and  $C_w$  expressed in decibels.

Expression (32) must be fulfilled by all of the nodes in the scenario, including those nodes belonging to the same cell ( $w = m$ ) and to the rest of cells ( $w \neq m$ ). According to (8), (32) may be written as

$$S_{m,n} < B_{m,n}^{w,l} + A_{m,n}^{w,l} + \Delta P_{P_m,w} + S_{w,l} \quad \{\forall w \in [0, \dots, M-1], \forall l \in [0, \dots, N_w-1], (w, l) \neq (m, n)\} \quad (33)$$

with  $A_{m,n}^{w,l} = \phi_{m,n}$  (in decibels)  $- \phi_{w,l}$  (in decibels),  $\Delta P_{P_m,w} = P_{P_m} - P_{P_w}$ , and  $B_{m,n}^{w,l} = \zeta \log(r_{w,l}/r_{m,n})$ .

It is worth noting that being connected to cell  $C_m$  is equivalent for a user to being connected to any of the  $N_m$  nodes of the cell  $C_m$ . In order to characterize this situation, the probability event  $\Gamma_{m,n}^{w,l}$  is defined as the condition that a user must fulfil in order to be connected to node  $\Omega_{m,n}$  instead of node  $\Omega_{w,l}$

$$\Gamma_{m,n}^{w,l} = \{S_{m,n} < B_{m,n}^{w,l} + A_{m,n}^{w,l} + \Delta P_{P_m,w} + S_{w,l}\}. \quad (34)$$

Accordingly, the probability  $P(Z_m \leq z)$  is the sum of the probability  $P(Z_{m,n} \leq z)$  for all nodes of  $C_m$  when the user is connected to  $\Omega_{m,n}$  and weighted for the probability of being connected to each node. Therefore,  $P(Z_m \leq z)$  is given by

$$P(Z_m \leq z) = \sum_{n=0}^{N_m-1} \left( P_{m,n}^{(1)} \cdot P_{m,n}^{(2)} \right) \quad (35)$$

where  $P_{m,n}^{(1)}$  is the probability  $P(Z_{m,n} \leq z)$  when it is known that  $\Gamma_{m,n}^{w,l} \{\forall w \in [0, \dots, M-1], \forall l \in [0, \dots, N_w-1], (w, l) \neq (m, n)\}$  is accomplished.

$$P_{m,n}^{(1)} = P(Z_{m,n} \leq z | \Gamma_{m,n}^{w,l}) = \frac{P(Z_{m,n} \leq z, \Gamma_{m,n}^{w,l})}{P(\Gamma_{m,n}^{w,l})} \quad (36)$$

and  $P_{m,n}^{(2)}$  is the probability of event  $\Gamma_{m,n}^{w,l}$ , knowing that the user is connected to cell  $C_m$  (or, equivalently, knowing that

event  $\Gamma_{m,n}^{w,l}$  is accomplished)

$$\begin{aligned}
 P_{m,n}^{(2)} &= P\left(\Gamma_{m,n}^{w,l} \left| \bigcup_{p=0}^{N_m-1} \Gamma_{m,p}^{w,l} \right.\right) \\
 &= \frac{P\left(\Gamma_{m,n}^{w,l} \bigcap_{p=0}^{N_m-1} \Gamma_{m,p}^{w,l}\right)}{P\left(\bigcup_{p=0}^{N_m-1} \Gamma_{m,p}^{w,l}\right)} \\
 &= \frac{P\left(\Gamma_{m,n}^{w,l}\right)}{P\left(\bigcup_{p=0}^{N_m-1} \Gamma_{m,p}^{w,l}\right)} \\
 &= \frac{P\left(\Gamma_{m,n}^{w,l}\right)}{\varphi_m} \tag{37}
 \end{aligned}$$

Assuming independence of lognormal shadowing ( $S_{m,n}$ ),  $P(Z_{m,n} \leq z, \Gamma_{m,n}^{w,l})$  results in

$$P(Z_{m,n} \leq z, \Gamma_{m,n}^{w,l}) = \int_{-\infty}^{s_{m,n}^0} \frac{e^{-\frac{s_{m,n}^2}{2\sigma_{S_{m,n}}^2}}}{\sqrt{2\pi}\sigma_{S_{m,n}}} \prod_{w=0}^{M-1} \prod_{l=0}^{N_w-1} \Lambda_{m,n}^{w,l} dS_{m,n} \tag{38}$$

$(w, l) \neq (m, n)$

where

$$s_{m,n}^0 = z + \phi_{m,n} - Y_0 - \zeta \log(r_{m,n}) \tag{39}$$

$$\Lambda_{m,n}^{w,l} = Q\left(\frac{S_{m,n} - B_{m,n}^{w,l} - A_{m,n}^{w,l} - \Delta P_{P_{m,w}}}{\sigma_{S_{w,l}}}\right) \tag{40}$$

$$\varphi_m = \sum_{n=0}^{N_m-1} \int_{-\infty}^{\infty} \frac{e^{-\frac{s_{m,n}^2}{2\sigma_{S_{m,n}}^2}}}{\sqrt{2\pi}\sigma_{S_{m,n}}} \prod_{w=0}^{M-1} \prod_{\substack{l=0 \\ (w,l) \neq (m,n)}}^{N_w-1} \Lambda_{m,n}^{w,l} dS_{m,n} \tag{41}$$

REFERENCES

[1] J. Shapira, "Microcell engineering in CDMA cellular networks," *IEEE Trans. Veh. Technol.*, vol. 43, no. 4, pp. 817–825, Nov. 1994.  
 [2] M. R. Bavafa and H. H. Xia, "Repeaters for CDMA systems," in *Proc. IEEE Veh. Technol. Conf.—Spring*, May 1998, vol. 2, pp. 1161–1165.  
 [3] J. Laiho, A. Wacker, and T. Novosad, *Radio Network Planning and Optimisation for UMTS*. Hoboken, NJ: Wiley, 2006.  
 [4] 3GPP TR 25.942, *Radio Frequency (RF) System Scenarios*, Mar. 2005.  
 [5] I. Chin-Lin, L. J. Greenstein, and R. D. Gitlin, "A microcell/macrocell cellular architecture for low- and high-mobility wireless users," *IEEE J. Sel. Areas Commun.*, vol. 11, no. 6, pp. 885–891, Aug. 1993.  
 [6] L. R. Hu and S. S. Rappaport, "Personal communication systems using multiple hierarchical cellular overlays," *IEEE J. Sel. Areas Commun.*, vol. 13, no. 2, pp. 406–415, Feb. 1995.  
 [7] B. Jabbari and W. F. Fuhrmann, "Teletraffic modeling and analysis of flexible hierarchical cellular networks with speed-sensitive handoff strategy," *IEEE J. Sel. Areas Commun.*, vol. 15, no. 8, pp. 1539–1548, Oct. 1997.  
 [8] J. Zhou and U. Yamamoto, "On the capacity and outage probability of a CDMA hierarchical mobile system with perfect/imperfect power control and sectorization," *IEICE Trans. Fundam. Electron. Commun. Comput. Sci.*, vol. E82-A, no. 7, pp. 1161–1170, Jul. 1999.  
 [9] J. S. Wu, J. K. Chung, and Y. C. Yang, "Performance study for a microcell hot spot embedded in CDMA macrocell systems," *IEEE Trans. Veh. Technol.*, vol. 48, no. 1, pp. 47–59, Jan. 1999.

[10] S. Kim, D. Hong, and J. Cho, "Hierarchical cell deployment for high speed data CDMA systems," in *Proc. IEEE Wireless Commun. Netw. Conf.*, Feb. 2002, pp. 7–10.  
 [11] J. Kim, Y. Han, and J. Ahn, "An adaptive traffic control scheme for hierarchically structured CDMA cellular systems," in *Proc. IEEE Veh. Technol. Conf.—Fall*, Sep. 2000, vol. 5, pp. 2192–2196.  
 [12] J. Y. Kim and G. L. Stuber, "Macrodiversity power control in hierarchical CDMA cellular systems," *IEEE J. Sel. Areas Commun.*, vol. 19, no. 2, pp. 266–276, Feb. 2001.  
 [13] M. Rahman and P. Erstrom, "Repeaters for hotspot capacity in DS-CDMA networks," *IEEE Trans. Veh. Technol.*, vol. 53, no. 3, pp. 626–633, May 2004.  
 [14] S. Kishore and L. J. Greenstein, "Capacity in a CDMA macrocell with a hotspot microcell: Exact and approximate analyses," in *Proc. IEEE Veh. Technol. Conf.—Fall*, Oct. 2001, vol. 2, pp. 1172–1176.  
 [15] A. H. Ali and J. G. Gardiner, "The performance of repeaters in UMTS networks," in *Proc. IEEE Mediterranean Electrotechnical Conf.*, May 2004, vol. 2, pp. 465–468.  
 [16] W. C. Y. Lee and D. J. Y. Lee, "The impact of repeaters on CDMA system performance," in *Proc. IEEE Veh. Technol. Conf.—Spring*, May 2000, vol. 3, pp. 1763–1767.  
 [17] QUALCOMM, *Repeaters for Indoor Coverage in CDMA Networks (white paper)*, 2003. [Online]. Available: <http://www.qualcomm.com/repeaterone>  
 [18] M. Rahman and P. Erstrom, "Repeaters for hotspot capacity in DS-CDMA networks," *IEEE Trans. Veh. Technol.*, vol. 53, no. 3, pp. 626–633, May 2004.  
 [19] W. Choi, B. Y. Cho, and T. W. Ban, "Automatic on-off switching repeater for DS/CDMA reverse link capacity improvement," *IEEE Commun. Lett.*, vol. 5, no. 4, pp. 138–141, Apr. 2001.  
 [20] T. W. Ban, B. Y. Cho, W. Choi, and H. S. Cho, "On the capacity of a DS/CDMA system with automatic on-off switching repeaters," in *Proc. IEEE Int. Conf. Commun.*, Jun. 2001, vol. 3, pp. 780–784.  
 [21] J. Niemela, P. Lahdekorpi, J. Borkowski, and J. Lempiainen, "Assessment of repeaters for WCDMA UL and DL performance in capacity-limited environment," in *Proc. IST Mobile Summit*, Jun. 2005.  
 [22] J. Borkowski, J. Niemela, and J. Lempiainen, "Applicability of repeaters for hotspots in UMTS," in *Proc. IST Mobile Summit*, Jun. 2005.  
 [23] F. Adellantado, J. Pérez-Romero, and O. Sallent, "Nonuniform traffic distribution model in reverse link of multirate/multiservice WCDMA-based systems," *IEEE Trans. Veh. Technol.*, vol. 56, no. 5, pp. 2902–2914, Sep. 2007.  
 [24] 3GPP TS 25.212, *Multiplexing and Channel Coding (FDD)*, Sep. 2005.  
 [25] J. Pérez-Romero, O. Sallent, R. Agustí, and M. A. Díaz-Guerra, *Radio Resource Management Strategies in UMTS*. Hoboken, NJ: Wiley, 2005.  
 [26] P. Lahdekorpi, J. Niemela, J. Borkowski, and J. Lempiainen, "WCDMA network performance in variable repeater hotspot traffic cases," in *Proc. IEE Int. Conf. 3G Beyond*, Nov. 2005, vol. 5, pp. 367–371.  
 [27] 3GPP TS 25.956, *Universal Terrestrial Radio Access (UTRA) Repeater Planning Guidelines and System Analysis*, Jan. 2005.  
 [28] 3GPP TS 25.106, *UTRA Repeater Radio Transmission and Reception*, Mar. 2006.  
 [29] 3GPP TS 25.143, *UTRA Repeater Conformance Testing*, Mar. 2006.  
 [30] K. S. Jeong, J. M. Cheong, T. H. Park, T. G. Kim, and S. Park, "Performance analysis of DS-CDMA reverse link with fiber-optic repeaters," in *Proc. IEEE Veh. Technol. Conf.—Spring*, May 2000, vol. 3, pp. 2439–2443.  
 [31] H. Holma and A. Toskala, *WCDMA for UMTS*. Hoboken, NJ: Wiley, 2007.  
 [32] F. Adellantado, O. Sallent, J. Pérez-Romero, and R. Agustí, "Impact of traffic hotspots in 3G W-CDMA networks," in *Proc. IEEE Veh. Technol. Conf.—Spring*, May 2004, vol. 4, pp. 2332–2336.



**Ferran Adellantado** (S'01–M'08) was born in Barcelona, Spain, in 1978. He received the Engineer of Telecommunications and Ph.D. degrees from the Universitat Politècnica de Catalunya, Barcelona, in 2001 and 2007, respectively.

He is currently with Universitat Oberta de Catalunya, Barcelona. He has been involved in projects funded by the European Union as well as in projects for private companies. His research interests include medium access control protocols and radio resource management techniques for wireless communication systems particularly in cognitive wireless networks.



**Jordi Pérez-Romero** (M'04) received the degree in telecommunications engineering and the Ph.D. degree from the Universitat Politècnica de Catalunya (UPC), Barcelona, Spain, in 1997 and 2001, respectively.

He is currently an Associate Professor with the Department of Signal Theory and Communications, UPC. He has been involved in different European projects as well as in projects for private companies. He has published papers in international journals and conferences and has coauthored one book on mobile communications. His research interests are in the field of mobile communication systems, particularly packet radio techniques, radio resource and quality of service management, heterogeneous wireless networks, and cognitive networks.



**Oriol Sallent** received the Engineer and Doctor Engineer degrees in telecommunication from the Universitat Politècnica de Catalunya (UPC), Barcelona, Spain, in 1994 and 1997, respectively.

He has been an Associate Professor with UPC since 1998. He has participated in many research projects and consultancies funded by either public organizations or private companies. His research interests are in the field of radio resource and spectrum management for heterogeneous cognitive wireless networks, where he has published more than 100 papers in IEEE journals and conferences.